Magnetic Sensor-Based Multi-Vehicle Data Association

Yimeng Feng, *Student Member, IEEE*, J. Andrew Zhang, *Senior Member, IEEE*, Bo Cheng, *Senior Member, IEEE*, Xiangjian He, *Senior Member, IEEE*, Junliang Chen, *Senior Member, IEEE*

Abstract—**Sensors have been playing an increasingly important role in smart cities. Using small roadside magnetic sensors provides a cost-efficient method for monitoring vehicle traffic. However, there are significant challenges associated with vehicle data misalignment due to the timing-offsets between sensors and missed or increased data because of vehicle lane-changing. In this paper, we propose a novel traffic information acquisition and vehicle state estimation scheme using multiple road magnetic sensors. To efficiently solve the multi-sensor registration problem in the presence of timing-offset, we develop a linear discrimination analysis method to achieve vehicle separation and classification. To handle the situation of lane-changing, we propose a data smoothing technique based on a multi-hypotheses tracker that exploits vehicle correlation. The road density effect on the probability of correct data association is investigated, with numerical and experimental results provided. The results show that our proposed scheme can effectively detect vehicles with a 95.5% accuracy rate. It also outperforms some other speed sensing methods in terms of the vehicle speed estimation accuracy.**
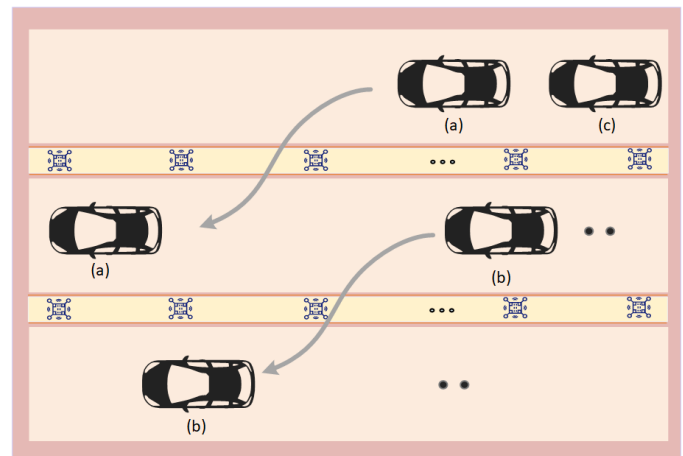
Index Terms—**data association, vehicle tracking, magnetic sensor**
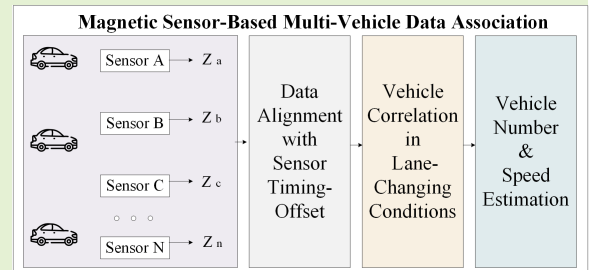
I. INTRODUCTION

SENSORS are used to make our world smart and connected [1]. It is becoming popular to use various sensors on roads, e.g., surveillance cameras, high precision LiDar and roadside portable sensors [2], [3]. With the large numbers of on-road vehicles and the measurements of uncertain sources, data association becomes a critical problem in vehicle detection. Because of the working mechanism of sensors, the measurements can come from the targets being tracked and non-desired clutter [4]. Moreover, a measurement often comes with a certain probability of false detection. The measurement likelihood is adopted to distinguish targets in clutter measurements and the clutter density is used to calculate the measurement likelihood ratio value [5].

Urban road surveillance can be implemented using magnetic sensors [6]. There are multiple works on using magnetic related sensors for vehicle detection and vehicle speed monitoring [7], [8]. A single magnetic sensor may be used for this purpose, as demonstrated in our previous work [9], where a

Y. Feng is with State Key Laboratory of Networking and Switching Technology, Beijing University of Posts and Telecommunications, Beijing, China, and she is also with the School of Electrical and Data Engineering, University of Technology Sydney, NSW, Australia. (e-mail: fyimeng@bupt.edu.cn).

J. Andrew Zhang and X. He are with the School of Electrical and Data Engineering, University of Technology Sydney, NSW, Australia. (e-mail: Andrew.Zhang@uts.edu.au; Xiangjian.He@uts.edu.au).

B. Cheng and J. Chen are with Beijing University of Posts and Telecommunications, Beijing, China.(e-mail: chengbo@bupt.edu.cn; chjl@bupt.edu.cn)

Fig. 1. An example shows the requirement of roadside magnetic sensor-based multi-vehicle data association. In the figure, the lanes are equipped with two lines of sensors. The processes of vehicle (a) driving from the upper lane to the middle lane is called birth-death processes in the Markov process. The birth-death processes create ambiguity in the magnetic sensor-based multi-vehicle data association. Moreover, they increase difficulties in vehicle tracking and state estimation.

tiny, cost-effective and environment-friendly magnetic sensor is used to separate vehicle magnetic signals and achieve vehicle speed estimation. The performance of successful vehicle detection and speed estimation may be significantly improved by using multiple magnetic sensors.

However, there are notable challenges with the use of multiple magnetic sensors. Fig. 1 is the illustration of a real road

situation. Time synchronization across sensors is one of the major problems here. It is generally inconvenient to achieve accurate time synchronization across sensors, which cause measurement ambiguity and challenges in data alignment. This is also known as the time registration problem. Moreover, tracking initialization in a dense environment suffers from the nonuniform data rate impact and data missing issue [10], as illustrated in Fig. 2. Although some works have been attempted, as will be reviewed in Section II, to the best of our knowledge, none of the current multiple-vehicle tracking solutions solves these issues at the same time.

This paper proposes a multi-magnetic-sensor based framework for vehicle detection and speed estimation to solve all the issues mentioned above. It is significantly extended from our previous work, as reported in a conference paper [11]. The proposed framework includes several major processing modules, including Linear Discrimination Analysis (LDA), Roadside Magnetometer Track-Oriented Multi-Hypotheses Tracker (RMTOMHT) in lane changing conditions, and performance analysis in a dense environment. The main contributions of this paper are as follows.

1) We propose an efficient roadside magnetometer track-oriented multiple hypotheses tracking solution that provides vehicle position and speed estimation based on the Kalman filter.

2) We propose an effective timing offset estimation and synchronization method for data fusion with multiple magnetic sensors, based on linear discriminant analysis;

3) Using collected experimental data, we evaluate the proposed scheme and show that it increases the fused detection precision by 95.5% compared to existing methods for vehicle detection using magnetic sensors. The theoretical and numerical results for association performance analysis are also shown to be well matched.

The rest of this paper is organized as follows. After a brief introduction of the related works in Section II, we formulate the vehicle association problem in the urban road environment in Section III. The major modules of the proposed scheme are presented in Section IV. We analyze the impact of the vehicle density on the probability of correct data association in Section V. The experimental analysis is provided in Sec. VI. And we conclude this paper and the potential work directions in Section VII.

II. RELATED WORK

In this section, we provide a brief review on existing works of magnetic sensor-based traffic surveillance, multiple object tracking methods, and asynchronous sensor fusion.

A. Traffic Surveillance Methods

In recent years, there are several works on traffic surveillance using magnetic related sensors [12]–[15]. Compared to other sensors, such as Camera, LiDar, and radar, using magnetic sensors can achieve a good balance between sensing performance and the deployment cost, with the additional advantages of working with most of weather and lighting conditions.
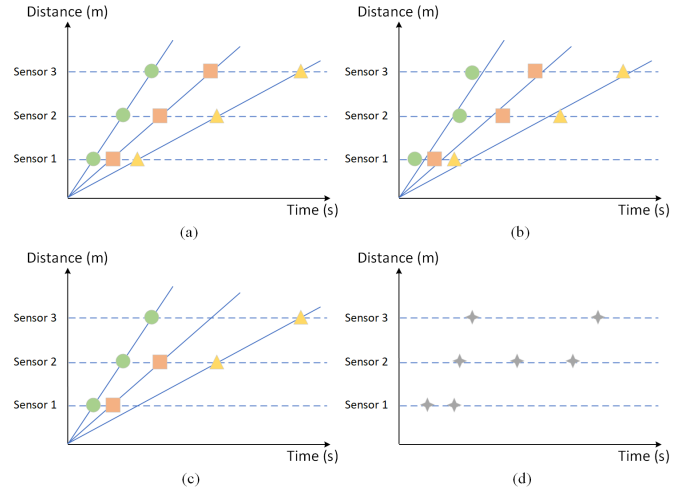

Fig. 2. An example shows the timing offset and missed measurement problems in a multi-sensor system for multi-vehicle tracking. The points of different shapes represent the measurements for various vehicles from the three magnetic roadside sensors. Fig. 2 (a) shows the ideal virtual tracks for the three cars in the absence of timing offset and missed measurements. Fig. 2 (b) shows the case with timing offset only. Fig. 2 (c) shows the case with missed measurements due to, e.g., vehicle changing lanes. Fig. 2 (d) depicts the measurements before being associated with target vehicles.

There have been some works on using mangetic related sensors for vehicle detection and tracking. Taghvaeeyan proposed a method using four magnetic sensors to count vehicles and estimate vehicle speeds in [8], with the result of 95% correct vehicle classification accuracy and less than 2.5% error over the entire range of 5-27 m/s in speed estimation. In [6], Wei and Yang adopted two magnetic sensors to estimate vehicle speed and another magnetic sensor for fusion, which resulted in a speed estimation accuracy of 80%. Vehicle acquisition and vehicle classification through an improved support vector machine classifier was proposed in [16] where magnetic signatures are used to identify vehicles of different lengths. However, the algorithm is complicated and require high processing capability to achieve 80% to 90% accuracy.

Magnetic loops have also been widely used for vehicle detection and speed estimation, e.g., as reported in [17]. Compared with magnetic loops, magnetic sensors three advantages. First, the working mechanism of magnetic loops are active, which create a inductive magnetic field to detect vehicels, but magnetic sensors don't. The magnetic sensors are passive sensors that only vibrate when vehicles pass. So the magnetic sensor won't disturb local magnetic fields like magnetic loops. Second, the installation and maintenance cost for magnetic loops are very high, but they only have a 3 to 5 years lifespan. While the magnetic sensor is much cheaper. Third, the installation of magnetic loops are not environmental-friendly as they need to be embedded under the road surface; while the magnetic sensors are small and easy to install.

B. Multiple Object Tracking Methods

With the development of modern surveillance systems, there are significant interests arising in the object tracking field [5], [18]. General estimation algorithms based on nearest

neighbour filter, which applies the nearest measurements for prediction, have limited performance in the environment where spurious measurements frequently occur. A pioneer work originally in [19] proposed to incorporate measurements for the uncertain origins into the existing track by applying a splitting strategy when more than one return was observed during the prediction. The split-track algorithm is applicable for tracking initiation and tracking update but the memory requirements and computational complexity increase quickly in dense environments. A simple clustering strategy using adjacency matrix, which encodes the neighborhood and connectivity of nodes in the network was proposed in [20]. The work in [21] applied scientific workflows in a container-based cloud for multi-agent task allocation, which reduced workflow makespans and traffic overheads through replicating tasks.

Jeng et al. in [22] proposed a side-view single-beam microwave vehicle detector system for estimating the speed and length of each vehicle. But their experiments target mainly at low-speed vehicles and lack of considering the mis-identified vehicles by radars because of high speeds and lane-changing. Hu et al. in [23] used fuzzy observer-based path-tracking control for autonomous vehicles. Li et al. in [24] used a novel smooth variable structure filter for target tracking under model uncertainty. Zhou et al. in [25] considered dynamic state estimation for a heavy vehicle. Authors in [26] used deep reinforcement learning trajectory control for target tracking but it was limited because of time consuming.

C. Asynchronous Measurements with Multiple Sensors

Several target tracking works have been proposed to deal with the asynchronous measurement problems [27]–[32]. In particular, the consensus random finite set approach for multi-object tracking is receiving increasing interests [33]. Authors in [34] proposed a fusion estimation method for multi-rate multi-sensor systems with missing measurements. Zhang's work [35] considered asynchronous sensor fusion estimators in a manoeuvring target tracking simulation, which shows that the local estimations are created in various time dimensions, and the numbers of local estimates from each sensor are time-varying. As shown in Fig. 3, sensor a and sensor b are of the same type of magnetic sensors with sampling rate $R_{sampling}$. We denote the cross-covariance $P_{a,b}$ from the estimated errors at the sensor a and sensor b. At times $t_{a,0}, t_{a,5}, t_{a,8}$, sensor a combines its estimations from sensor b to get the fused estimates. At instants $t_{a,1}, t_{a,2}, t_{a,3}, t_{a,4}, t_{a,6}, t_{a,7}$, the measurements from sensor b are blank, so sensor b remains its own estimations as to the combined value. $P_{a,b}$ calculates only at times $t_{a,0}, t_{a,5}, t_{a,8}$, where $t_{ab,0} = t_{a,0} = t_{b,0}, t_{ab,1} = t_{a,5} = t_{b,3}$, and $t_{ab,2} = t_{a,8} = t_{b,5}$, so that P_{ab} is updated with a non-uniform rate. To a group of sensors whose measurement rates are asynchronous, the core solution is to allow all sensors to obtain the same estimates by using some consensus algorithms. But the object density issue is not considered in a cluttered environment.

Our work is distinctive from the traffic surveillance works reviewed above. In this paper, our proposed multi-vehicle tracking and state estimation method are cost-efficient, multi-sensor based and measurement-oriented. We process the
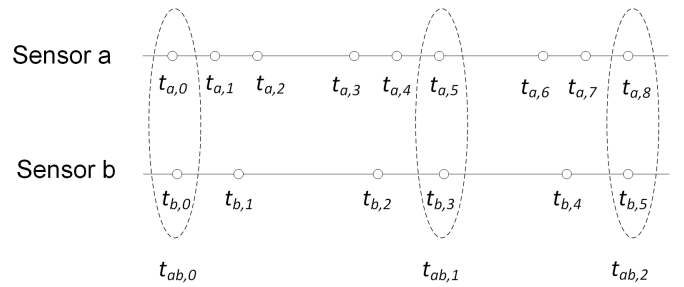

Fig. 3. An asynchronous sensor fusion illustration.

measurements from roadside magnetic sensors to detect the numbers and speeds of vehicles, and align the sensor time registration to improve vehicle separation and classification. Moreover, we consider the complex, dense road situation in a lane-changing situation. Overall, our work provides a novel method for reliable and high-precision vehicle state estimation.

III. Multi-Vehicle Data Association Problem

In this section, the formal definition of the problem is given. Assume that N_s sensors are installed on the roadside, and a number of vehicles drive by the sensors. The vehicle is assumed to drive along the road, which is a relatively constrained environment. Besides, because the measurement timeframes for each car by the sensors are pretty short (basically between 1–3s), it is reasonable to assume that the vehicles travel at a nearly constant speed. Thus, the motion is represented by a simple 1-D constant velocity motion model given that a vehicle i remains on the same lane when they across the roadside sensors, at a constant speed v_i. We set the first sensor to start from position x_0. The motion is represented by a 1-D constant velocity motion model given by

$$\mathbf{x}_t = \begin{bmatrix} 1 & T_s \\ 0 & 1 \end{bmatrix} \mathbf{x}_{t-1} + \begin{bmatrix} \frac{T_s}{2} \\ T_s \end{bmatrix} \bar{a}, \tag{1}$$

where the discrete-time index is defined as $t = 1, 2, ..., T$, T_s is the sampling time, and $\bar{a}$ is the average acceleration and in our model it equals to zero.

Adding the measurement noise n, the observations y are related to the state vector $\mathbf{x_t}$ by the relation

$$y = f(\mathbf{x}_t) + n. \tag{2}$$

where n is the value of the observational noise, $f(\mathbf{x}_t)$ is the coordinate transformations to predict an observation.

The i-th vehicle drives at speed v_i. n_i is the actual vehicle number and p_i is the detected number of vehicles. The main purpose of multi-vehicle tracking is to design an estimator for estimating p_i to minimize the Root Mean Squared Error (RMSE) and Mean Absolute Percentage Error (MAPE) of the estimates, which are defined by

$$\text{RMSE} = \sqrt{\frac{\sum_{i=1}^{N_s} |n_i - p_i|^2}{N_s}}, \tag{3}$$

$$\text{MAPE} = \frac{1}{N_s} \sum_{i=1}^{N_s} \frac{|n_i - p_i|}{p_i}. \tag{4}$$
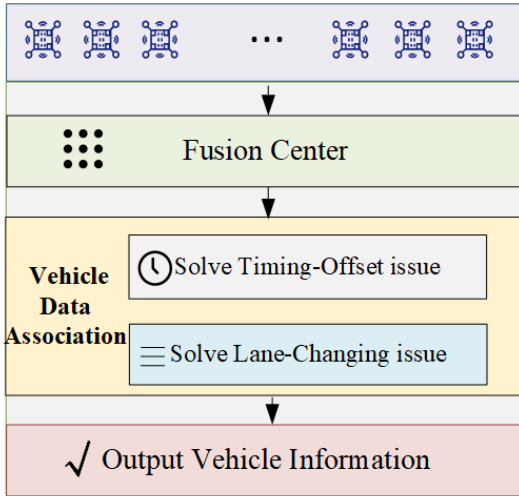
Fig. 4. The framework of our proposed scheme.

Our goal is to exploit all magnetic sensors' measurements to achieve accurate vehicle detection and speed estimation. We present the framework of our proposed scheme in Fig. 4. Firstly, we collect the measurements of sensors into the fusion center. Secondly, we achieve magnetic sensor-based multi-vehicle data association, including solving the timing-offset issue and solving the lane changing issue. Then, we output the vehicle information such as the estimated vehicle number and vehicle speeds. The vehicle speed can be obtained through the travel time of an identified vehicle between different sensors.

IV. KEY TECHNOLOGIES IN THE FRAMEWORK

The architecture of the magnetic sensor-based multi-vehicle data association system is shown in Fig. 5. First, the passive roadside sensors record timestamps when vehicles pass by the sensors. The measurements are then processed in two modules: the data alignment process and vehicle correction process. In this section, the two modules are illustrated in detail.

A. Data Alignment with Sensor Timing-Offset

Due to the hardware limitations, the reported data from sensors can result in timing offset between sensors. As shown in Fig. 2, the subplot (a) with ideal measurements becomes (b) in the presence of timing-offset; With the consideration of missed data due to lane-changing it becomes (c).

A multiple-sensor based tracking method need to be developed to resolve the problem of time alignment. Here, we propose to use a method to classify the reported data and eliminate timing-offset effect. Since the sensor measurements are from vehicles in their constant speeds and the proposed magnetic sensor framework possesses the same linear characteristics with the measurements, we base the time registration method on the LDA technique to detect and separate measured vehicles. LDA in [36] uses statistical and machine learning methods to find a linear classifier for dimension reduction, which is derived from the optimal Bayes classifier when classes are assumed to be Gaussian distributed with identical

covariance matrices. The measurements are processed from the classifier and the timing-offset effect disappears after the processing. Thus we can realize data alignment for vehicle detection.

Since each vehicle drives independently, we can assume that each vehicle category has a mean u_i and covariance Σ. Then, the scatter between the categories can be defined by the sample covariance of the category means as

$$\Sigma_b = \frac{1}{N} \sum_{i=1}^{N} (\mu_i - \mu)(\mu_i - \mu)^T, \tag{5}$$

where μ is the mean of the category means. The wiehin-class scatter matrix S in the $\vec{w}$ direction, in this case, is given by

$$S = \frac{\vec{w}\Sigma_b\vec{w}}{\vec{w}^T\Sigma\vec{w}}. \tag{6}$$

This equation means if $\vec{w}$ is an eigenvector of $\Sigma^{-1}\Sigma_b$, the division equals to the corresponding eigenvalue. Therefore, LDA can classify the data into its closest class.

B. Vehicle Correlation in Lane-Changing Conditions

There is a need to consider the situation when vehicles change lanes on roads with several lanes [37]–[40]. When this happens, measurements for the vehicles can be lost from one sensor and/or appear in another sensor, due to limited sensing distance. Such reduced or increased measurements can cause a wrong association in the vehicle datasets. Only using the LDA classifier in Section IV. A cannot achieve high accuracy in such a complex environment. This problem can be mitigated by using more magnetic sensors or sensors with longer working ranges, at increased infrastructure costs. Alternatively, we use advanced signal processing techniques to smooth the measurements and track vehicles and vehicle states.

One of such techniques is to estimate the unknown vehicle driving tracks based on prior knowledge such as the vehicle start location and the moving speed. Only the vehicle moving direction is assumed to be known, and the moving speed is introduced as an unknown constant. Here, based on the multiple-hypothesis tracking theory in [41], we propose a method called Roadside Magnetometer Track-Oriented Multi-Hypotheses Tracker (RMTOMHT) to estimate the next track based on prior tracks. We improve the multiple-hypothesis in vehicle tracking and extend it in using advanced roadside magnetic sensors, where the working mechanism is shown in Fig. 6. The proposed tracker works by combining the roadside magnetic sensors' detecting results and vehicle moving characteristics.

The goal of RMTOMHT is to find the best M associations θ_k^m and prune all other $\theta_k \in \Theta_k$ through each update. In Fig. 8, the data inputs include an RMTOMHT tracker and vehicle states with two fields, the means and covariance of initial vehicle states. For each local hypothesis in each hypothesis tree, we first implement gating validation in the ellipsoidal area and remove the measurements that do not fall inside any local hypothesis gate. Then, we calculate the missed detection and
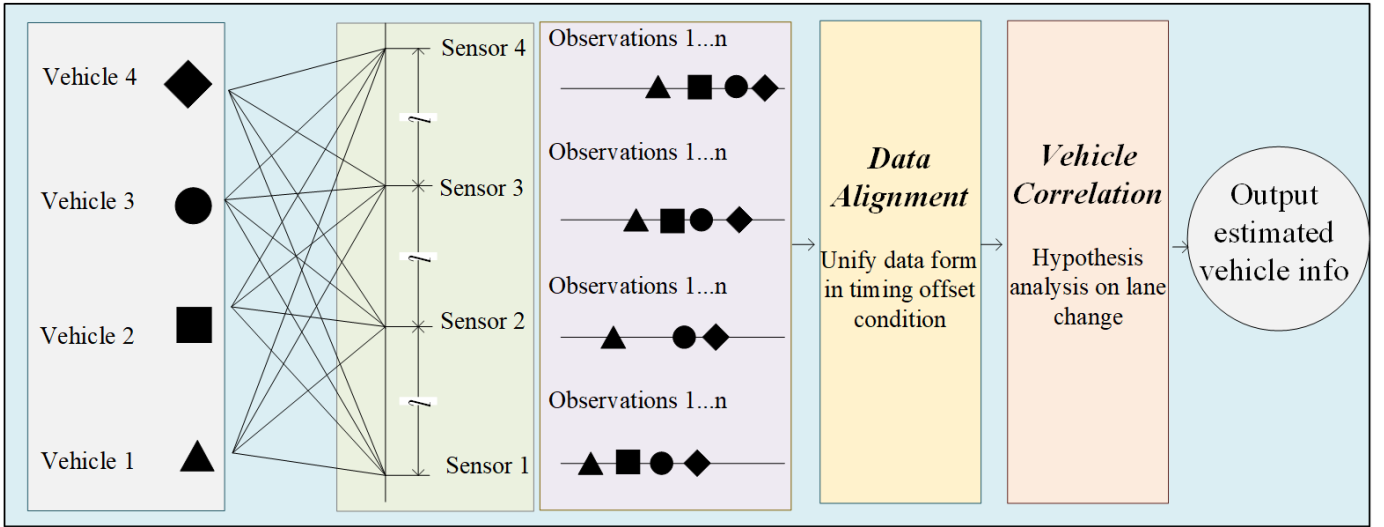
Fig. 5. The proposed magnetic sensor-based multi-vehicle data association architecture.

predicted likelihood for each measurement inside the gate and save these for future use. We then update the local hypotheses and save them, connecting them to the old hypotheses and the new measurements. For each predicted global hypothesis, we start with creating a cost matrix, then by using the Hungarian algorithm, we can obtain M best assignments. By updating the global hypothesis table according to the M best assignment matrix and using new local hypothesis indexing, we then normalize the weights of the global hypothesis and apply candidate reduction technique: pruning and capping. Prune means to cut off local hypotheses that are not included in any of the global hypothesis trees. Then, we re-index the global hypothesis at the look-up table and output the object state estimates from the global hypothesis with the highest weight. Finally, we predict each local hypothesis in every hypothesis tree.

The mathematical representations used in the tracker is described as follows. First, to evaluate the estimated state $\hat{\mathbf{x}}_{\mathbf{k}} =< \mathbf{x}_{\hat{i},\mathbf{k}}, \mathbf{v}_{\hat{i},\mathbf{k}} >$ of $\mathbf{x}_k$ from the vehicle i, we define

$$\tilde{\mathbf{x}}_{\mathbf{k}} = \mathbf{x}_{\mathbf{k}} - \hat{\mathbf{x}}_{\mathbf{k}}, \tag{7}$$

and its covariance matrix by

$$\mathbf{P}_{k|k} = \mathbf{E}\left[\left(\mathbf{x}_{\mathbf{k}} - \mathbf{x}_{\hat{\mathbf{k}|\mathbf{k}}}\right)\left(\mathbf{x}_{\mathbf{k}} - \mathbf{x}_{\hat{\mathbf{k}|\mathbf{k}}}\right)' | \mathbf{z}_{\mathbf{k}}\right]$$

$$= \mathbf{E}\left[\tilde{\mathbf{x}}_{\mathbf{k}} \tilde{\mathbf{x}}_{\mathbf{k}}'\right]. \tag{8}$$

The normalized and squared state estimation error is then given by

$$\varepsilon_{\mathbf{k}} = \mathbf{x}_{\mathbf{k}} \tilde{\mathbf{P}}_{k|k}^{-1} \tilde{\mathbf{x}}_{\mathbf{k}}. \tag{9}$$

The filtering process follows that

$$\mathbf{x}_{\mathbf{k+1}} = \mathbf{\Phi}\mathbf{x}_{\mathbf{k}} + \mathbf{w}_{\mathbf{k}}, \tag{10}$$

where $\mathbf{\Phi}$ is the state transition model that is applied to the next state, $\mathbf{w}_{\mathbf{k}}$ is the process noise and is assumed to follow a

zero-mean multivariate normal distribution. The measurement $\mathbf{z}_k$ is related to the state vector $\mathbf{x}_k$ via

$$\mathbf{z}_{\mathbf{k}} = \mathbf{H}\mathbf{x}_{\mathbf{k}} + \mathbf{v}_{\mathbf{k}}. \tag{11}$$

where $\mathbf{v}_{\mathbf{k}}$ is the observation noise and is assumed to be zero mean Gaussian white noise.

The process noise covariance is $\mathbf{Q}_{\mathbf{k}} = \mathbf{E}[\mathbf{w}_{\mathbf{k}}\mathbf{w}_{\mathbf{k}}']$ and the observation noise covariance is $\mathbf{R}_{\mathbf{k}} = \mathbf{E}[\mathbf{v}_{\mathbf{k}}\mathbf{v}_{\mathbf{k}}']$. Denote the innovations variance matrix $\mathbf{S}_{\mathbf{k}}$ by

$$\mathbf{S}_{\mathbf{k}} = \mathbf{Q}_{\mathbf{k}} + \mathbf{R}_{\mathbf{k}}. \tag{12}$$

The hypothesis construction is based on the Cramer-Rao lower bound (CRLB), which is the convariance matrix of the target estimate $\hat{\mathbf{x}}$ and is defined by

$$\mathbf{E}\left[\tilde{\mathbf{x}}_{\mathbf{k}}\tilde{\mathbf{x}}_{\mathbf{k}}'\right] \geqslant \boldsymbol{J}^{-1}, \tag{13}$$

where

$$\boldsymbol{J} = \mathbf{E}\left\{\left[\nabla_x ln\Lambda\left(x\right)\right]\left[\nabla_x ln\Lambda\left(x\right)\right]'\right\}|_{\mathbf{x}=\mathbf{x}_0}, \tag{14}$$

and $\boldsymbol{J}$ is the Fisher information matrix (FIM). The measurements are $\{z_k\}$ and the likelihood function of the target parameter $\Lambda\left(x\right)$ is defined by

$$\Lambda\left(x\right) = p\left(Z^n|\mathbf{x}\right) = p\left[z\left(1\right),...z\left(n\right)|\mathbf{x}\right]. \tag{15}$$

Then, for the hypothesis validation process, the Gaussian procedure is used for selecting measurements $\{\mathbf{z}_k\}$ from the elliptical area, where the measurement prediction is $\hat{\mathbf{z}_k}$ and the innovation variance matrix is $\mathbf{S}_{\mathbf{k}}$. The validation region allows to eliminate the measurements that are statistically far away from the estimated vehicle positions. These estimates are calculated with the gate threshold γ, which can be obtained from the standard distribution table. The validation gate is defined as [42]

$$[\mathbf{z}_{\mathbf{k}} - \hat{\mathbf{z}_{\mathbf{k}}}]'\mathbf{S}_{\mathbf{k}}^{-1}[\mathbf{z}_{\mathbf{k}} - \hat{\mathbf{z}_{\mathbf{k}}}] \leq \gamma. \tag{16}$$
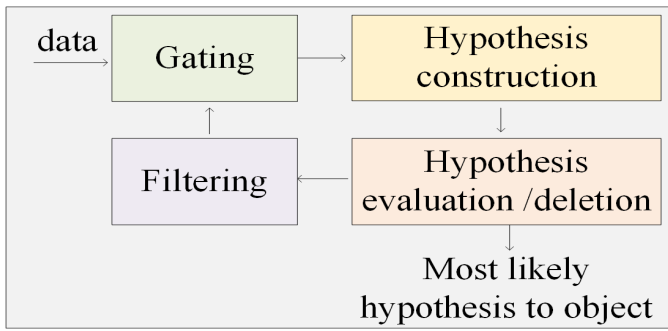
Fig. 6.   RMTOMHT working mechanism.

Algorithm 1 The multi-vehicle data association algorithm.

Input :   The unified data $S_1, S_2, ..., S_n$ from magnetic
        sensors S.

Output :   Detected vehicle numbers n

  1: **if** consistent vehicle data in S

  2:      Get the correlation of vehicles through classification
algorithm in Sec. IV. A

  3: **else**

  4:      Do lane change analysis

  5:      Estimate vehicle moving tracks in Sec IV. B

  6: **end**

  7: calculate detected vehicle numbers n

After several iterations, the most likely hypothesis to the vehicles is obtained.

C. Summary of Multi-Vehicle Data Association

Here, we summarize the proposed technique that uses multiple sensors to detect multiple on-road driving vehicles in Algorithm 1. The algorithm can efficiently handle the timing offset that may result in vehicle misclassification and the complex lane change situations. In particular, we apply LDA to achieve successful vehicle classification and use RMTOMHT for vehicle state estimation and data smoothing, as described in Sec. IV. A and Sec. IV. B, respectively.

V. SIMULATION RESULTS AND PERFORMANCE ANALYSIS

The accuracy of vehicle data association is sensitive to the density of vehicles on the road. This section conducts simulation results in Sec. IV. and a theoretical analysis on the impact of vehicle density on the performance of vehicle data association.

A. Simulation Results

To verify the proposed LDA for vehicle classification, we conduct numerical experiments using Matlab 2019b of the multi-sensor tracking driving vehicle scenario. In this scenario, we simulate ten magnetic sensors with a distance of 10m in line and three vehicles passing by the sensors at a minimum time difference of 2s. The speed of the following vehicle is not larger than the previous one. Note that the timing offset is significantly smaller than the interval of vehicles passing by the same sensor, and they have constant and small
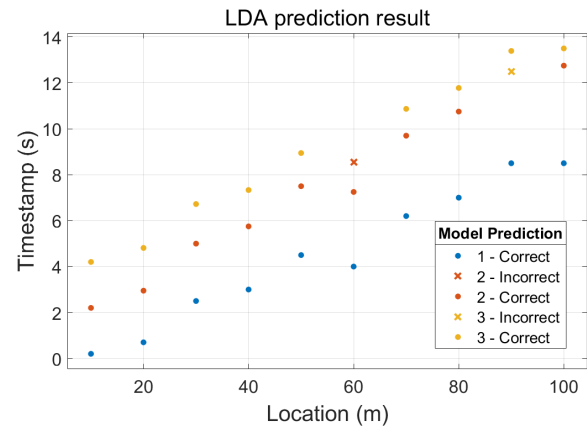

Fig. 7.   The LDA prediction result for three vehicles. Different vehicles are represented in different colours. Dots are for correct predictions and crosses are for incorrect predictions.
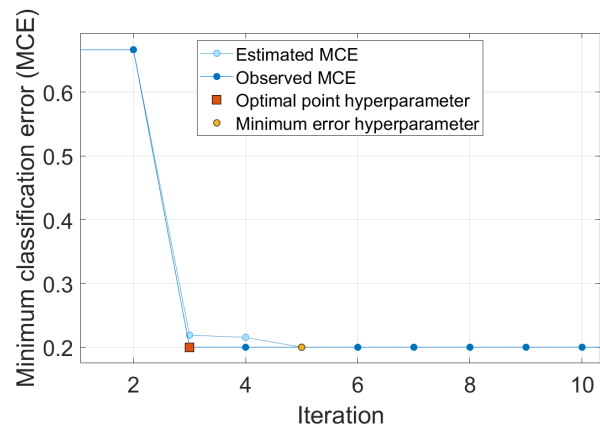

Fig. 8.   The minimum classification error (MCE) of applying LDA in vehicle classification with time offset.

values with absolute values smaller than 50ms in each sensor. The prediction results obtained by LDA are compared with the true vehicle locations, as shown in Fig. 7, where a correct prediction means that the predicted data matches the real data. As can be seen from the results, LDA achieves a good prediction result with a 93.3% accuracy.

To further test the effectiveness of LDA, we use cross-validation, where we split the data set into ten folds and each fold is used as a testing set at some point. In the first iteration, we test the model, and we train the model using the rest. In the second fold, we use the second fold as the test group, and the rest as the training group. Repeat the process until each fold is used as the testing set. The Mahalanobis distance, which measures the distance between data points and their distribution, is used to measure the accuracy here.

Fig. 8 shows how the estimated minimum classification errors (MCE) varies with different iterations. Through each iteration, the MCEs are reduced. In particular, at the third iteration, the model reached an optimal point hyperparameter and at the fifth iteration, the minimum error hyperparameter is achieved. We can also see that the estimated MCE matches well with the actually observed MCE, which are the true values of MCE.
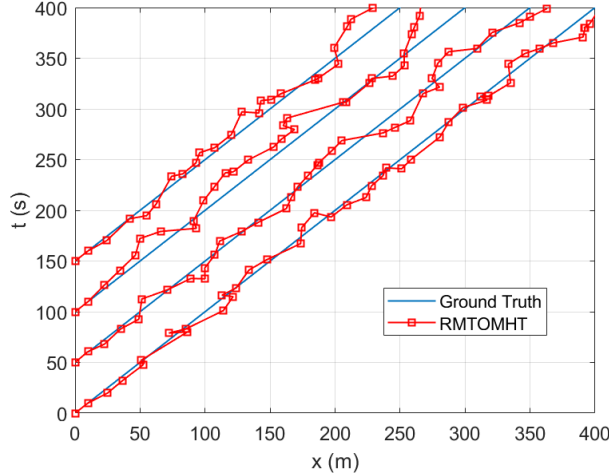
Fig. 9. Ground truth vs the results obtained by RMTOMHT. The red squares are the estimated four-vehicle movement results that combine locations and speeds by applying the aforementioned tracking and fusion rules. Four blue lines are ground truths for the four simulated vehicles driving on the road.

Here, we conduct a simulation to validate the proposed tracker using Matlab 2019b on a computer with Windows 10 operation system. The initial state settings for the vehicles are $\mathbf{x}_{1,1} = \begin{bmatrix} 0 & 20 \end{bmatrix}^T$, $\mathbf{x}_{2,1} = \begin{bmatrix} 50 & 20 \end{bmatrix}^T$, $\mathbf{x}_{3,1} = \begin{bmatrix} 100 & 20 \end{bmatrix}^T$, $\mathbf{x}_{4,1} = \begin{bmatrix} 150 & 20 \end{bmatrix}^T$. That is, the prior speed is 20m/s for each vehicle and the initial location of each vehicle is $\begin{bmatrix} 0m & 50m & 100m & 150m \end{bmatrix}$. At different time t, the estimated values are obtained in each state according to the proposed tracker. As can be seen from Fig. 9, the estimated results of RMTOMHT match well with the ground truth, and they demonstrate that RMTOMHT can effectively track vehicle driving when the vehicle could not be detected in the lane changing situation.

B. Probability of Correct Data Association

One of the important considerations in multi-vehicle tracking is the impact of the vehicle density β on the probability of correct data association, such as the method proposed in Section IV. Assume that there are N objects and N is a Poisson random variable with mean ν. The vehicle density is defined as the expected number of vehicles in the O_m volumn of the m-unit measurement space with radius r, and can be represented by

$$\beta = \frac{\nu}{O_m r^m}. \tag{17}$$

We introduce the probability of correct association P_C and the average tracking innovation variance $\bar{\sigma}$ ($\bar{\sigma} = \sqrt{S}$) to evaluate the density effect in vehicle tracking systems. Then, the probability of the actually existing objects can be expressed by

$$P_N = e^{-\nu} \frac{\nu^N}{N!}. \tag{18}$$

The correct association probability P_C is originally formulated in [43] for N object tracking, and is given by

$$P_C = \sum_{N=0}^{\infty} P\{\hat{q}_i = q_i | N\} P_N$$

$$\approx e^{-\nu} \left\{ 1 + \sum_{N=1}^{\infty} \left[1 - \tilde{C}_m \left(\frac{\bar{\sigma}}{r} \right)^m \right]^{N-1} \frac{\nu^N}{N!} \right\}$$

$$= \frac{e^{-\nu \tilde{C}_m \left(\frac{\bar{\sigma}}{r} \right)^m} - \tilde{C}_m \left(\frac{\bar{\sigma}}{r} \right)^m e^{-\nu}}{1 - \tilde{C}_m \left(\frac{\bar{\sigma}}{r} \right)^m}$$

$$\approx exp\left[-\nu \tilde{C}_m \left(\frac{\bar{\sigma}}{r} \right)^m \right] = exp\left[\tilde{C}_m \tilde{\beta} \right]$$

$$= exp\left[-\tilde{C}_m \beta \bar{\sigma}^m \right], \tag{19}$$

where $\tilde{C}_m$ is a constant and is defined as $\tilde{C}_m = 2^{m-1} \pi^{-\frac{1}{2}} \Gamma\left(\frac{m+1}{2} \right)$, and Γ is the gamma function. Here, C_m is a constant, defined by

$$C_m = O_m \tilde{C}_m = 2^{m-1} \pi^{(m-1)/2} \frac{\Gamma\left(\frac{m+1}{2} \right)}{\Gamma\left(m/2 + 1 \right)}$$

$$= \begin{cases} \frac{1}{2} \pi^{m/2} \frac{m!}{[(m/2)!]^2} & \text{if } m \text{ is even} \\ 2^{2m} \pi^{(m/2)-1} \frac{[(m-1)/2]![(m+1)/2]!}{(m+1)!} & \text{if } m \text{ is odd} \end{cases}, \tag{20}$$

Here, we consider $m = 1$, which represents that the measurements are from vehicles driving on a straight lane.

C. Numerical Analysis

Fig. 10 shows the results of correct association probability analysis through Monte Carlo simulations. Because we consider vehicle driving in a straight line, which is in a 1-D environment, the dimension of the observation space is one (i.e., $m = 1$). According to the correct association probability equations, we have $C_1 = 2\pi^{-\frac{1}{2}}$, then $P_c = exp(-\frac{2}{\sqrt{\pi}} \cdot \beta \cdot (\bar{\sigma})^{\frac{2}{\sqrt{\pi}}})$. According to Mori's contribution to the probability of correct association, we use default values for other parameters in [43]. The point results shown in Fig. 10 are obtained by averaging over 50 independent samples obtained in Monte Carlo simulations. The estimated vehicle number N is 100 and the variance Q and R are set to be diagonal matrices. As can be seen from Fig. 10, the simulation results match well with the theoretical analysis, except for a few values when the densities are as high as 0.50.

VI. EVALUATION

In this section, we present the results for the proposed vehicle tracking method with real road experiments using roadside magnetic sensors. We start by introducing the experimental setup, and then present our vehicle detection results and compare them with the work in [44] and [45].
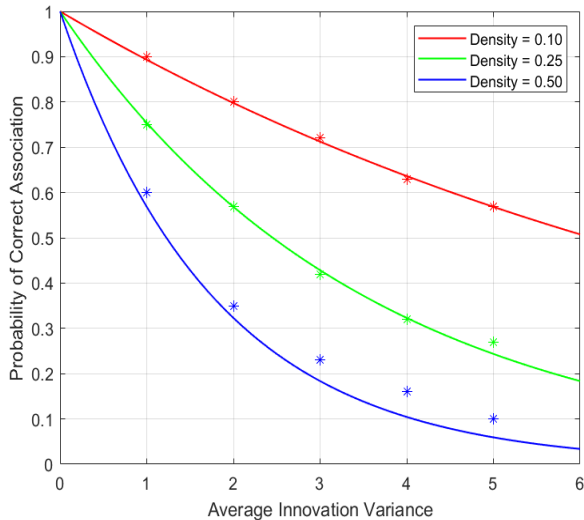
Fig. 10. Correct association probability as average innovations variance $\bar{\sigma}$ in 1-D environment.

Fig. 12. The surf diagram from the measurements of sensors in Experiment 1.

Fig. 11. A camera recorded driving scene of real experiments with magnetic sensors on the roadside.

A. Experimental Setup

The experiment was conducted at a lane using a line of nine RM3100 magnetic sensors on the roadside. Each magnetic sensor was installed on the roadside at a distance of 10m, as shown in Fig. 11. Multiple types of vehicles were present in the experiments, and their impacts on measurement accuracy of magnetic sensors were investigated in our previous work [46] and are not considered in this paper. We recorded timestamps when vehicles drove by the sensors. All RM3100 magnetic sensord have the same sampling rate of 100Hz, and their timing offsets are unknown. Note that although the targeted lane was the one closest to the roadside, the sensor could also detect some long, heavy trucks driving on the roadside's other lanes, since their magnetic response was relatively small compared to the vehicles driving in the target lane. All measured vehicles were driving in one direction. We used a video camera to record road situations and manually counted the actual vehicle numbers accurately as ground truth. Fig. 11 is a screenshot from the video, where the camera was put in the same place as the first magnetic sensor.
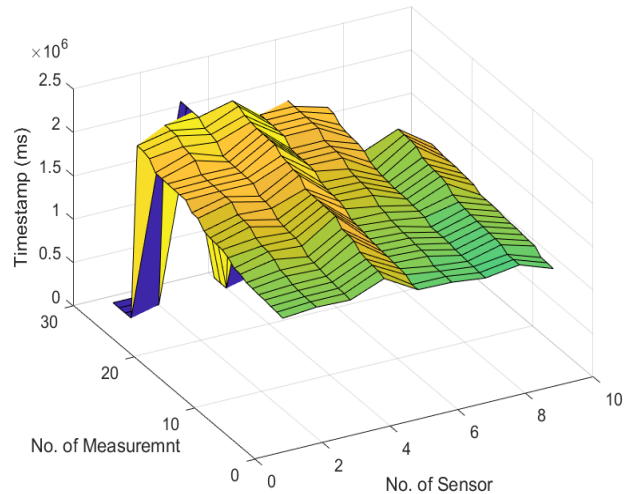
B. Vehicle Association Results and Analysis

We conducted two on-road experiments to test the developed scheme. The speeds of the vehicles being tested are under 60km/h, the speed limit of the roads. The data was processed individually for each experiment, and the data are visually shown as the surf diagrams in Fig. 12 and Fig. 13, respectively. We processed the sensor measurements to estimate the number of vehicles in each experiment. Each diagram displays the measurements in three dimensions: the sequence of the sensors, the number of measurements, and vehicle detection timestamps. The missed values are filled with 0 as in the figures. The results of vehicle detection were presented in Table. 1. We define the correct rate (detection accuracy) as $\left|\frac{No.Detect-No.Actual}{No.Actual}\right|$. The actual numbers of vehicles in Experiment 1 and Experiment 2 are 28 and 49, respectively. We can see that the overall sensor fusion has stable detection rates of 92.9% and 95.5%. For comparison, the work in [44] has vehicle recognition rates of 89.5% and 92.86%, respectively. Furthermore, if we increase the number of samples, the successful vehicle recognition rate can be further improved, where the vehicle density and road innovation variance remain the same in the short period. Besides, different weather conditions were confronted in the experiments, such as sunny and light rain, but no heavy rain. No obvious impact of weather conditions on the results is observed. From Table I, we can also see that some sensors alone have relatively large missed detections and low accuracy, such as sensor 8, primarily due to environmental noise. This shows the importance of aggregating multi-sensor measurements for vehicle detection. We also compare our proposed detection results with direct measurements in Fig. 14 and Fig. 15 for the two experiments. As can be seen from the figures, our proposed detection method outperforms the method without combining LDA and RMTOMHT.

Fig. 16 plots the cumulative distribution function (CDF) of the vehicle speed estimation errors (km/h) for our proposed
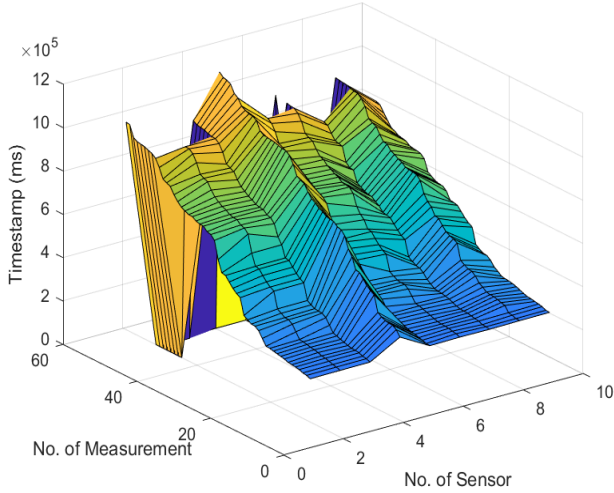
Fig. 13. The surf diagram from the measurements of sensors in Experiment 2.

TABLE I
CORRECT VEHICLE DETECTION RESULTS

Sensors	Experiment 1		Experiment 2	
	No. Detection	Accuracy	No. Detection	Accuracy
1	25	89.3%	51	95.9%
2	26	92.6%	43	87.8%
3	29	96.4%	49	100%
4	26	92.6%	50	98%
5	27	96.4%	45	92.8%
6	28	100%	48	98%
7	27	96.4%	46	93.9%
8	22	78.6%	51	95.9%
9	24	85.7%	48	98%
Avg	**26**	**92.9%**	**47**	**95.5%**

estimation method. For comparison, the results obtained by the Derivative Dynamic Time Warping (DDTW) method [41] [47] and GPS are also provided. The results demonstrate that as a cost-effective solution, our method achieves much better speed estimation performance. For example, for our method, 90% of estimation errors are lower than 8km/h, and 50% of estimation errors are less than 2.5km/h. In addition, only 1% of the estimated speed errors exceeds 10km/h. As a comparison, 80% of DDTW's estimation errors are lower than 9km/h. Compared to some state-of-the-art results using other sensors, such as magnetic loops, our method may have slightly inferior results. However, our method has the advantages of easy deployment and relatively low cost. Compared to work in [45] using magnetic sensors, our method achieves a higher detection rate of 95.5%, with a margin of 3.2%. We also list our speed estimation results against the reference speeds in Fig. 17. The estimated speed are very close to the reference speed, which validates our proposed tracking method.

For vehicles driving at higher speeds, although the experiments were not done, we can expect degraded performance for two reasons: (1) Magnetic sensors have some difficulties in detecting high-speed vehicles as reported in [19]; and (2) according to the analysis in Section V.B, higher-speed
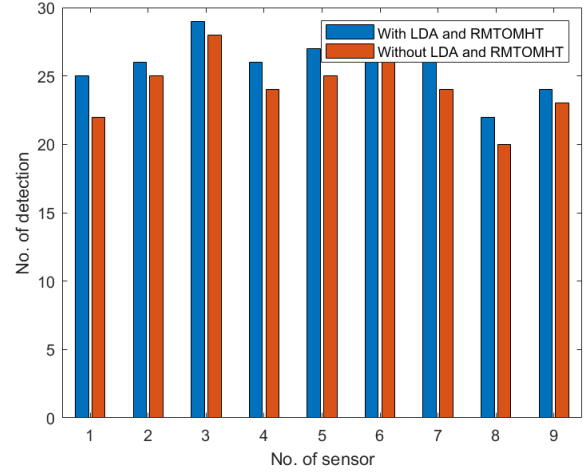

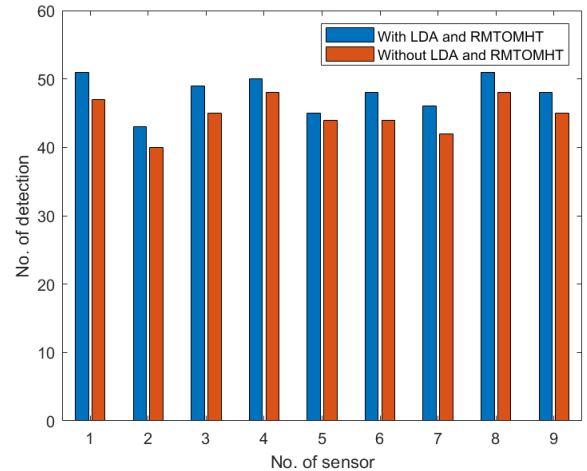Fig. 14. The vehicle detection results in Experiment 1.

Fig. 15. The vehicle detection results in Experiment 2.

vehicles result in higher innovation variance, which decreases the correct association probability.

VII. CONCLUSION

This paper investigates the on-road vehicle detection problem and proposes a tracking framework with the use of roadside magnetic sensors. The framework consists of two main modules, data alignment for handling sensor timing offset and vehicle correlation method for smoothing measurements in the case of lane switching. The linear discrimination analysis was first applied to remove timing offset and align the measurements from multiple sensors. The vehicle correlation hypothesis was then established and associated with estimated vehicle locations. We also studied the probability of correct association as a function of vehicle density. Numerical and experimental results validate the effectiveness of our proposed scheme.

During the design and implementation of the scheme, we also found that the scheme did not function very well in the cases of, e.g., frequent lane switching in a multi-lane environment. This may be resolved via jointly processing signals from
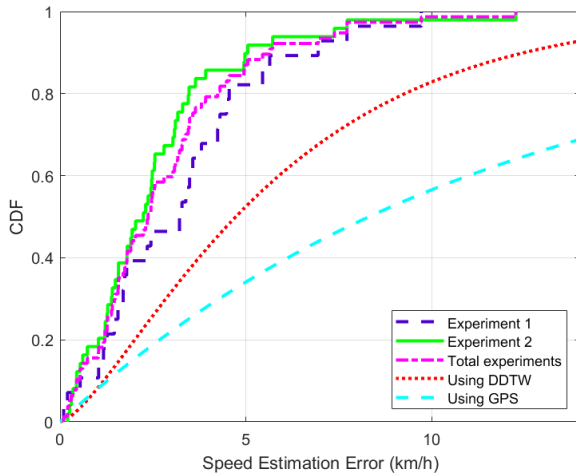
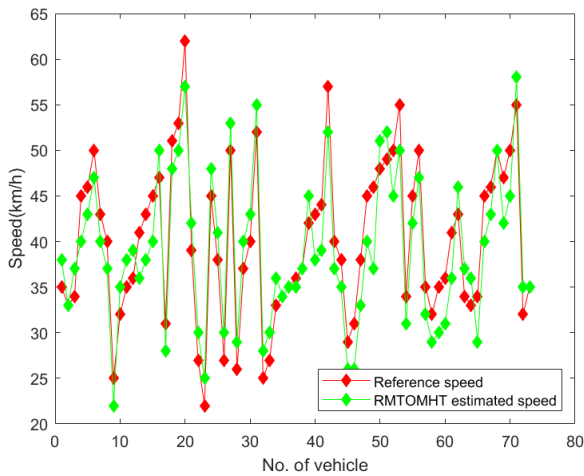Fig. 16. The CDF of the estimated speeds using multiple sensors.

Fig. 17. The comparison of estimated speeds and reference speeds.

sensors deployed for different lanes. The proposed framework can in principle be applied to any road, however, the cost will increase with the number of lanes increasing. Thus one important ongoing research is to enable the use of one sensor for multiple lanes. It is also worthwhile to enhance solutions by fusing the magnetic sensors with other traffic sensors, e.g., high precision LiDar and camera-based road sensing approaches. In addition, overlapped measurements may be recorded if two cars crash in one lane. Such cases may be investigated and identified via analysing magnetic vibrations from sensors, which vary with the distances to vehicles. Deployment of multiple magnetic sensors on different lanes is suggested when analysing overlapping transportation issues.

ACKNOWLEGMENT

REFERENCES

[1] A. C. Jose and R. Malekian, "Improving smart home security: Integrating logical sensing into smart home," *IEEE Sensors Journal*, vol. 17, no. 13, pp. 4269–4286, 2017.

[2] W. Balid, H. Tafish, and H. H. Refai, "Intelligent vehicle counting and classification sensor for real-time traffic surveillance," *IEEE Transactions on Intelligent Transportation Systems*, vol. 19, no. 6, pp. 1784–1794, 2018.

[3] Q. Wang, J. Zheng, H. Xu, B. Xu, and R. Chen, "Roadside magnetic sensor system for vehicle detection in urban environments," *IEEE Transactions on Intelligent Transportation Systems*, vol. 19, no. 5, pp. 1365–1374, 2018.

[4] R. O. Chavez-Garcia and O. Aycard, "Multiple sensor fusion and classification for moving object detection and tracking," *IEEE Transactions on Intelligent Transportation Systems*, vol. 17, no. 2, pp. 525–534, 2016.

[5] A. Chakraborty, A. Das, and A. K. Roy-Chowdhury, "Network consistent data association," *IEEE Transactions on Pattern Analysis and Machine Intelligence*, vol. 38, no. 9, pp. 1859–1871, 2016.

[6] Q. Wei and B. Yang, "Adaptable vehicle detection and speed estimation for changeable urban traffic with anisotropic magnetoresistive sensors," *IEEE Sensors Journal*, vol. 17, no. 7, pp. 2021–2028, 2017.

[7] K. Garg, N. Ramakrishnan, A. Prakash, and T. Srikanthan, "Rapid and robust background modeling technique for low-cost road traffic surveillance systems," *IEEE Transactions on Intelligent Transportation Systems*, vol. 21, no. 5, pp. 2204–2215, 2020.

[8] S. Taghvaeeyan and R. Rajamani, "Portable roadside sensors for vehicle counting, classification, and speed measurement," *IEEE Transactions on Intelligent Transportation Systems*, vol. 15, no. 1, pp. 73–83, 2014.

[9] Y. Feng, G. Mao, B. Cheng, B. Huang, S. Wang, and J. Chen, "Magspeed: A novel method of vehicle speed estimation through a single magnetic sensor," in *2019 IEEE Intelligent Transportation Systems Conference (ITSC)*, Conference Proceedings, pp. 4281–4286.

[10] W. Li and L. Henry, "Simultaneous registration and fusion of multiple dissimilar sensors for cooperative driving," *IEEE Transactions on Intelligent Transportation Systems*, vol. 5, no. 2, pp. 84–98, 2004.

[11] L. Wan, G. Chen, and Y. Feng, "Multi-vehicle tracking and state estimation through data association," in *SAE Technical Paper*, 2020, Conference Proceedings, pp. 1–7.

[12] X. Chen, X. Kong, M. Xu, K. Sandrasegaran, and J. Zheng, "Road vehicle detection and classification using magnetic field measurement," *IEEE Access*, vol. 7, pp. 52 622–52 633, 2019.

[13] H. Dong, X. Wang, C. Zhang, R. He, L. Jia, and Y. Qin, "Improved robust vehicle detection and identification based on single magnetic sensor," *IEEE Access*, vol. 6, pp. 5247–5255, 2018.

[14] A. Haoui, R. Kavaler, and P. Varaiya, "Wireless magnetic sensors for traffic surveillance," *Transportation Research Part C: Emerging Technologies*, vol. 16, no. 3, pp. 294–306, 2008.

[15] Z. Papp, J. Sijs, and M. Lagioia, "Sensor network for real-time vehicle tracking on road networks," in *2009 International Conference on Intelligent Sensors, Sensor Networks and Information Processing (ISSNIP)*, Conference Proceedings, pp. 85–90.

[16] J. Lan, Y. Xiang, L. Wang, and Y. Shi, "Vehicle detection and classification by measuring and processing magnetic signal," *Measurement*, vol. 44, no. 1, pp. 174–180, 2011.

[17] F. Mocholi Belenguer, A. Mocholi Salcedo, A. Guill Ibanez, and V. Milian Sanchez, "Advantages offered by the double magnetic loops versus the conventional single ones," *PLOS ONE*, vol. 14, no. 2, pp. 1–6, 2019. [Online]. Available: https://dx.doi.org/10.1371/journal.pone.0211626

[18] X. Fan, C. Xiang, C. Chen, P. Yang, L. Gong, X. Song, P. Nanda, and X. He, "Buildsensys: Reusing building sensing data for traffic prediction with cross-domain learning," *IEEE Transactions on Mobile Computing*, pp. 1–1, 2020.

[19] R. W. Sittler, "An optimal data association problem in surveillance theory," *IEEE transactions on military electronics*, vol. 8, no. 2, pp. 125–139, 1964.

[20] W. Dargie and J. Wen, "A simple clustering strategy for wireless sensor networks," *IEEE Sensors Letters*, vol. 4, no. 6, pp. 1–4, 2020.

[21] M. Niu, B. Cheng, Y. Feng, and J. Chen, "Gmta: A geo-aware multi-agent task allocation approach for scientific workflows in container-based cloud," *IEEE Transactions on Network and Service Management*, vol. 17, no. 3, pp. 1568–1581, 2020.

[22] S.-L. Jeng, W.-H. Chieng, and H.-P. Lu, "Estimating speed using a side-looking single-radar vehicle detector," *IEEE transactions on intelligent transportation systems*, vol. 15, no. 2, pp. 607–614, 2014.

[23] C. Hu, Y. Chen, and J. Wang, "Fuzzy observer-based transitional path-tracking control for autonomous vehicles," *IEEE Transactions on Intelligent Transportation Systems*, vol. 22, no. 5, pp. 3078–3088, 2021.

[24] Y. Li, G. Li, Y. Liu, X. P. Zhang, and Y. He, "A novel smooth variable structure filter for target tracking under model uncertainty," *IEEE Transactions on Intelligent Transportation Systems*, pp. 1–17, 2021.

[25] S. Zhou, H. Zhao, W. Chen, Z. Liu, H. Wang, and Y. Liu, "Dynamic state estimation and control of a heavy tractor-trailers vehicle," *IEEE/ASME Transactions on Mechatronics*, pp. 1–1, 2020.

[26] J. Moon, S. Papaioannou, C. Laoudias, P. Kolios, and S. Kim, "Deep reinforcement learning multi-uav trajectory control for target tracking," *IEEE Internet of Things Journal*, pp. 1–1, 2021.

[27] S. Sun, N. Akhtar, H. Song, A. S. Mian, and M. Shah, "Deep affinity network for multiple object tracking," *IEEE transactions on pattern analysis and machine intelligence*, 2019.

[28] J. Zhu, H. Yang, N. Liu, M. Kim, W. Zhang, and M.-H. Yang, "Online multi-object tracking with dual matching attention networks," in *Proceedings of the European Conference on Computer Vision (ECCV)*, 2018, Conference Proceedings, pp. 366–382.

[29] P. Chu and H. Ling, "Famnet: Joint learning of feature, affinity and multi-dimensional assignment for online multiple object tracking," in *Proceedings of the IEEE International Conference on Computer Vision*, 2019, Conference Proceedings, pp. 6172–6181.

[30] M. Tang, Y. Rong, J. Zhou, and X. R. Li, "Information geometric approach to multisensor estimation fusion," *IEEE Transactions on Signal Processing*, vol. 67, no. 2, pp. 279–292, 2018.

[31] M. Kordestani, A. Chibakhsh, and M. Saif, "A control oriented cyber-secure strategy based on multiple sensor fusion," in *2019 IEEE International Conference on Systems, Man and Cybernetics (SMC)*, Conference Proceedings, pp. 1875–1881.

[32] D. Smith and S. Singh, "Approaches to multisensor data fusion in target tracking: A survey," *IEEE Transactions on Knowledge and Data Engineering*, vol. 18, no. 12, pp. 1696–1710, 2006.

[33] K. Da, T. Li, Y. Zhu, H. Fan, and Q. Fu, "Recent advances in multisensor multitarget tracking using random finite set," *Frontiers of Information Technology & Electronic Engineering*, vol. 22, no. 1, pp. 5–24, 2021.

[34] M. Kordestani, M. Dehghani, B. Moshiri, and M. Saif, "A new fusion estimation method for multi-rate multi-sensor systems with missing measurements," *IEEE Access*, vol. 8, pp. 47 522–47 532, 2020.

[35] W.-A. Zhang, S. Liu, M. Z. Chen, and L. Yu, "Fusion estimation for two sensors with nonuniform estimation rates," in *2012 IEEE 51st IEEE Conference on Decision and Control (CDC)*. IEEE, Conference Proceedings, pp. 4083–4088.

[36] A. M. Martinez and A. C. Kak, "Pca versus lda," *IEEE Transactions on Pattern Analysis and Machine Intelligence*, vol. 23, no. 2, pp. 228–233, 2001.

[37] S. Moridpour, M. Sarvi, and G. Rose, "Lane changing models: a critical review," *Transportation letters*, vol. 2, no. 3, pp. 157–173, 2010.

[38] R. S. Tomar, S. Verma, and G. S. Tomar, "Neural network based lane change trajectory predictions for collision prevention," in *2011 International Conference on Computational Intelligence and Communication Networks*, Conference Proceedings, pp. 559–564.

[39] Y. Liu, X. Wang, L. Li, S. Cheng, and Z. Chen, "A novel lane change decision-making model of autonomous vehicle based on support vector machine," *IEEE Access*, vol. 7, pp. 26 543–26 550, 2019.

[40] J. Feng, J. Ruan, and Y. Li, "Study on intelligent vehicle lane change path planning and control simulation," in *2006 IEEE International Conference on Information Acquisition*, Conference Proceedings, pp. 683–688.

[41] S. Coraluppi and C. A. Carthel, "If a tree falls in the woods, it does make a sound: multiple-hypothesis tracking with undetected target births," *IEEE Transactions on Aerospace and Electronic Systems*, vol. 50, no. 3, pp. 2379–2388, 2014.

[42] Y. Bar-Shalom, T. E. Fortmann, and P. G. Cable, *Tracking and data association*. Acoustical Society of America, 1990.

[43] Y. Bar-Shalom, "Multitarget-multisensor tracking: advanced applications," *Norwood, MA, Artech House, 1990, 391 p.*, 1990.

[44] J. Lan, Y. Xiang, L. Wang, and Y. Shi, "Vehicle detection and classification by measuring and processing magnetic signal," *Measurement*, vol. 44, no. 1, pp. 174–180, 2011.

[45] B. Yang and Y. Lei, "Vehicle detection and classification for low-speed congested traffic with anisotropic magnetoresistive sensor," *IEEE Sensors Journal*, vol. 15, no. 2, pp. 1132–1138, 2014.

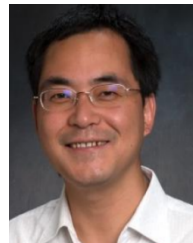[46] Y. Feng, G. Mao, B. Cheng, C. Li, Y. Hui, Z. Xu, and J. Chen, "Mag-monitor: Vehicle speed estimation and vehicle classification through a magnetic sensor," *IEEE Transactions on Intelligent Transportation Systems*, pp. 1–12, 2020.

[47] G. Chandrasekaran, T. Vu, A. Varshavsky, M. Gruteser, R. P. Martin, J. Yang, and Y. Chen, "Tracking vehicular speed variations by warping mobile phone signal strengths," in *2011 IEEE International Conference on Pervasive Computing and Communications (PerCom)*. IEEE, Conference Proceedings, pp. 213–221.

Yimeng Feng (S'19) received the B.S. degree from Beijing University of Posts and Telecommunications, Beijing, China and Queen Mary University of London, London, the United Kingdom, in 2016. She is currently pursuing the dual Ph.D. degree program with State Key Laboratory of Networking and Switching Technology, Beijing University of Posts and Telecommunications, Beijing, China, and the School of Electrical and Data Engineering, University of Technology Sydney, NSW, Australia. Her current research interests include data science in Internet of Things, intelligent transportation systems and wireless sensor network technology.

J. Andrew Zhang (M'04-SM'11) received the B.Sc. degree from Xi'an JiaoTong University, China, in 1996, the M.Sc. degree from Nanjing University of Posts and Telecommunications, China, in 1999, and the Ph.D. degree from the Australian National University, in 2004. Currently, Dr. Zhang is an associate Professor in the School of Electrical and Data Engineering, University of Technology Sydney, Australia. He was a researcher with Data61, CSIRO, Australia from 2010 to 2016, the Networked Systems, NICTA, Australia from 2004 to 2010, and ZTE Corp, Nanjing, China from 1999 to 2001. Dr. Zhang's research interests are in the area of signal processing for wireless communications and sensing, and autonomous vehicular networks. He has published more than 190 papers in leading international Journals and conference proceedings, and has won 5 best paper awards for his work. He is a recipient of CSIRO Chairman's Medal and the Australian Engineering Innovation Award in 2012 for exceptional research achievements in multigigabit wireless communications.

Bo Cheng received the Ph.D. degree in computer science and engineering from the University of Electronic Science and Technology of China, in 2006. He has been with the Beijing University of Posts and Telecommunications (BUPT) since 2008. He is currently a Full Professor with the Research Institute of Networking Technology, BUPT. His current research interests include network services and intelligence, Internet of Things technology, and multimedia communications.

Xiangjian He received the Ph.D. degree in computer science from the University of Technology Sydney (UTS), Ultimo, NSW, Australia, in 1999. He is currently a Full Professor and the Director of the Computer Vision and Pattern Recognition Laboratory, Global Big Data Technologies Centre, UTS.

Junliang Chen received the B.S. degree in electrical engineering from Shanghai Jiao Tong University, China, in 1955, and the Ph.D. degree in electrical engineering from the Moscow Institute of Radio Engineering, in 1961. He has been with the Beijing University of Posts and Telecommunications (BUPT) since 1955. He is currently the Chairman and a Professor with the Research Institute of Networking and Switching Technology, BUPT. His research interests are in the area of communication networks and next generation service creation technology. He was elected as a member of the Chinese Academy of Science in 1991 and the Chinese Academy of Engineering in 1994.